

Phase separation in star-polymer–colloid mixtures

J. Dzubiella,* A. Jusufi, C. N. Likos, C. von Ferber, and H. Löwen

Institut für Theoretische Physik II, Heinrich-Heine-Universität Düsseldorf, Universitätsstraße 1, D-40225 Düsseldorf, Germany

J. Stellbrink,^{1,2} J. Allgaier,¹ D. Richter,¹ A. B. Schofield,² P. A. Smith,² W. C. K. Poon,² and P. N. Pusey²

¹*IFF-Neutronenstreuung, Forschungszentrum Jülich GmbH, D-52425 Jülich, Germany*

²*Department of Physics and Astronomy, The University of Edinburgh, Mayfield Road, Edinburgh EH9 3JZ, United Kingdom*

(Received 12 October 2000; published 21 June 2001)

We examine the demixing transition in star-polymer–colloid mixtures for star arm numbers $f=2,6,16,32$ and different star-polymer–colloid size ratios $0.18 \leq q \leq 0.50$. Theoretically, we solve the thermodynamically self-consistent Rogers-Young integral equations for binary mixtures using three effective pair potentials obtained from direct molecular computer simulations. The numerical results show a spinodal instability. The demixing binodals are approximately calculated and found to be consistent with experimental observations.

DOI: 10.1103/PhysRevE.64.010401

PACS number(s): 82.70.Dd, 61.20.Gy, 64.70.–p

Typical soft matter systems, such as polymers and colloids, almost always occur in the form of mixtures. It is the central goal of soft matter physics to offer insights into the generic phase behavior of such systems, which do not depend on the detailed chemical structure of their constituents. In this respect, the study of mixtures of hard colloidal particles and nonadsorbing polymer *chains* has received a great deal of recent attention, both experimentally [1–3] and theoretically [3–6]. The theoretical approaches to the study of colloid-polymer mixtures were largely based on the Asakura-Oosawa (AO) model, in which the chains are envisaged as noninteracting spheres experiencing a hard-sphere repulsion with the colloids. This model is most pertinent for Θ -like solvent conditions for the polymer. It can be mapped onto an effective one-component fluid featuring the so-called depletion interaction between the colloids, mediated by the ideal chains [3,4] and leading to fluid-fluid separation at polymer-colloid size ratios exceeding the value $q_c \cong 0.30$. Though the AO model provides an excellent benchmark for such systems, recent theoretical studies [5,6] and comparisons with experiments [2] indicate that the assumption of noninteracting chains lead to quantitative discrepancies between the two. Hence, a systematic effort to derive more realistic chain-chain [7] as well as chain-colloid [6,8] interactions has already been undertaken.

On the opposite end of the polymer-colloid mixture lies the binary hard-sphere (BHS) mixture of large and small colloidal particles. Here, no fluid-fluid separation takes place [9]. It is therefore desirable to consider systems that interpolate between the AO and the BHS models, in order to systematically investigate the evolution of the phase behavior as we move from one extreme case to the other. Mixtures of colloids and nonadsorbing *star polymers* in a good solvent are such a natural bridge. Stars consist of f chains covalently attached on a common center, covering the range from simple chains ($f=1$ or 2) to stiff particles for large functionality f [10–12]. In this paper, we employ recently derived analytical expressions for the star-polymer–star polymer and

star-polymer–colloid interactions for all f values and for a large range of size ratios between the two [13]. Using these expressions, we make theoretical predictions on the mixing-demixing (or “gas-liquid”) transition in star-polymer–colloid mixtures and on their systematic dependence on the stiffness f and the size ratio of the two components. Our measured demixing curves are in good agreement with the theoretical predictions.

We consider a binary system with N_c colloidal spheres of diameter σ_c (radius R_c) and N_s star polymers, characterized by a diameter of gyration σ_g (radius of gyration R_g) and an arm number f . The total particle number is $N=N_c+N_s$. Let $q=\sigma_g/\sigma_c$ be the size ratio and $\eta_c=(N_c/V)(\pi/6)\sigma_c^3$ and $\eta_s=(N_s/V)(\pi/6)\sigma_g^3$ the packing fractions of the colloids and stars respectively, in the volume V .

Experimentally, we studied two sets of star-polymer–colloid mixtures consisting of poly(methylmethacrylate) (PMMA) particles and poly(butadiene) (PB) star polymers with size ratios $q \approx 0.49$ and $q \approx 0.18$, respectively. PMMA particles were synthesized following a standard procedure [14]. Stock suspensions were prepared either in *cis*-decahydronaphthalene (*cis*-decalin) or *cis*-decalin/tetrahydronaphthalene (tetralin) mixture as an index-matched solvent. These systems have been established as hard sphere models [1]. The volume fraction η_c was calibrated using the onset of the hard sphere freezing transition, taken to be at $\eta_c=0.494$ and observed as the nucleation of iridescent colloidal crystals. The PB star polymers were prepared by anionic polymerization following an established procedure [15,16]. Star arms were synthesized by polymerizing butadiene with secondary butyl lithium as the initiator. The resulting living polymer chains were coupled to the chlorosilane linking agent having ideally 6, 16, and 32 Si-Cl-groups. The molecular weights M_w of the PB arms were adjusted to give star polymers with values of $\langle R_g^2 \rangle^{1/2} = 0.0172 M_w^{0.609} f^{-0.403}$ [17] as close to 50 nm as possible. A linear PB polymer ($f=2$) was prepared as a reference system. The particles and star polymers were characterized using light and small angle neutron scattering (SANS) [18]. The results are summarized in Table I.

*Email address: joachim@thphy.uni-duesseldorf.de

TABLE I. Molecular characteristics of PMMA particles and PB star polymers.

Monomer	f	M_w (10^{-6} g/Mol) ^a	R_c (nm) ^b	R_g (nm) ^a
PMMA	—	—	104.0 ± 2.5	—
PMMA	—	—	289.0 ± 4.5	—
PB	2	0.86 ± 0.36	—	51.0 ± 3.5
PB	6	1.51 ± 0.06	—	52.1 ± 0.6
PB	16	3.45 ± 0.27	—	51.1 ± 0.5
PB	32	5.11 ± 0.39	—	51.4 ± 0.5

^aSmall angle neutron scattering (SANS).^bStatic light scattering (SLS).

Samples were prepared by mixing PMMA suspensions with PB stock solutions. Each sample was homogenized by prolonged tumbling and allowed to equilibrate and observed by eye at room temperature $T=25^\circ\text{C}$ [19]. In all samples with $q \approx 0.49$, the addition of polymer to suspensions with $\eta_c \sim 0.1-0.4$ brought about, successively, phase separation into colloidal gas and liquid (or demixing), triple coexistence of gas, liquid, and crystal, and gas-crystal coexistence. In samples with $q \approx 0.18$, the addition of polymer first led to fluid-crystal coexistence; a metastable gas-liquid binodal buried inside the equilibrium fluid-crystal coexistence region was encountered at higher polymer concentrations [20]. In all cases, demixing started within several hours and crystallization within two days. Here we focus on the demixing transition.

Theoretically we model the thermodynamics of the mixtures on the level of pair potentials between the two mesoscopic components, having integrated out the monomer and solvent degrees of freedom. Thus, three pair potentials are used as inputs for thermodynamically self-consistent integral equations, which are closed with the Rogers-Young (RY) scheme [21]. The colloid-colloid interaction at center-to-center distance r is taken to be that of hard spheres (HS)

$$V_{cc}(r) = \begin{cases} \infty, & r \leq \sigma_c \\ 0, & \text{else.} \end{cases} \quad (1)$$

The effective interaction between two stars in a good solvent was recently derived by theoretical scaling arguments, and verified by neutron scattering and molecular simulation, where the monomers were explicitly resolved [11,12]. The pair potential is modeled by an ultrasoft interaction that is logarithmic for an inner core and shows a Yukawa-type exponential decay at larger distances [11,22],

$$V_{ss}(r) = \frac{5}{18} k_B T f^{3/2} \times \begin{cases} -\ln\left(\frac{r}{\sigma_s}\right) + \frac{1}{1 + \sqrt{f}/2} & r \leq \sigma_s \\ \frac{\sigma_s/r}{1 + \sqrt{f}/2} \exp\left[-\frac{\sqrt{f}}{2\sigma_s}(r - \sigma_s)\right] & \text{else,} \end{cases} \quad (2)$$

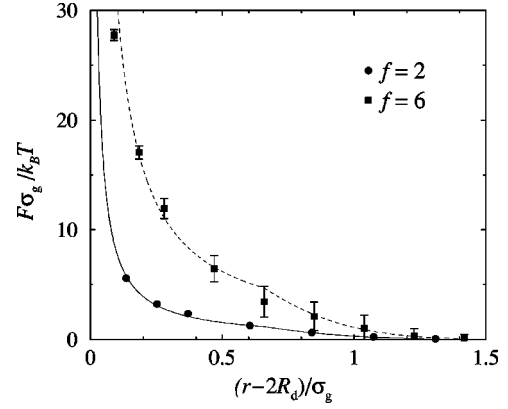


FIG. 1. Effective force between two isolated star polymers for arm numbers $f=2,6$ at center-to-center distance r . The theoretical result (line) derived from Eq. (3) is compared to computer simulation data (symbols) to obtain the decay parameter τ . R_d is the nonvanishing core radius of one simulated star, the values in Table II. Error bars are shown for the case $f=6$ and provide an estimate for all f values.

with $k_B T$ being the thermal energy. Our computer simulations show that the so-called corona-diameter σ_s remains fixed for all considered arm numbers f , being related to the diameter of gyration through $\sigma_s \approx 0.66\sigma_g$ [12]. However, the theoretical approach giving rise to Eq. (2) does not hold for arm numbers $f \lesssim 10$, because the Daoud-Cotton model of a star [23], on which the Yukawa decay rests, is not valid for small f . In these cases, the interaction inclines to a shorter-ranged decay for $r > \sigma_s$. This is consistent with approaches that at the linear polymer limit a Gaussian behavior of the pair potential is predicted [7,8,24]. Only the large distance decay of the interaction is affected; its form at close approaches has to remain logarithmic [25]. Accordingly, we propose the following star-star pair potential for arm numbers $f \lesssim 10$, replacing the Yukawa by a Gaussian decay,

$$V_{ss}(r) = \frac{5}{18} k_B T f^{3/2} \times \begin{cases} -\ln\left(\frac{r}{\sigma_s}\right) + \frac{1}{2\tau^2\sigma_s^2} & r \leq \sigma_s \\ \frac{1}{2\tau^2\sigma_s^2} \exp[-\tau^2(r^2 - \sigma_s^2)] & \text{else,} \end{cases} \quad (3)$$

where $\tau(f)$ is a free parameter of the order of $1/R_g$ and is obtained by fitting to computer simulation results; see Fig. 1 and Table II. Using $\tau\sigma_s(f=2) = 1.03$, we obtain for the second virial coefficient of polymer solutions the value $B_2/R_g^3 = 5.59$, in agreement with the estimate $5.5 < B_2/R_g^3 < 5.9$ from the renormalization group and the simulations [8].

An analytic form for the star-polymer–colloid pair potential can be found by integrating the osmotic pressure of one star along the spherical surface of a colloid, following an idea put forward by Pincus [26]. This can be achieved for arbitrary curvatures of the colloid, but the analytical result below is accurate for size ratios $q \lesssim 0.7$ and reads [13],

$$V_{sc}(r) = \Lambda k_B T f^{3/2} \frac{\sigma_c}{2r} \times \begin{cases} \infty & r < \frac{\sigma_c}{2}; \\ \xi_2 - \ln\left(\frac{2z}{\sigma_s}\right) - \left(\frac{4z^2}{\sigma_s^2} - 1\right) \left(\xi_1 - \frac{1}{2}\right) & \frac{\sigma_c}{2} \leq r < \frac{\sigma_s + \sigma_c}{2}; \\ \xi_2 [1 - \text{erf}(2\kappa z)] / [1 - \text{erf}(\kappa\sigma_s)] & \text{else,} \end{cases} \quad (4)$$

where $z = r - \sigma_c/2$ is the distance from the center of the star polymer to the surface of the colloid. The constants are $\xi_1 = 1/(1 + 2\kappa^2\sigma_s^2)$ and $\xi_2 = (\sqrt{\pi}\xi_1/\kappa\sigma_s)\exp(\kappa^2\sigma_s^2)[1 - \text{erf}(\kappa\sigma_s)]$. $\Lambda(f)$ and $\kappa(f)$ are fit parameters, obtained from computer simulations where the force between an isolated star and a hard flat wall is calculated (see Fig. 2). κ is in the order of $1/\sigma_g$ (see the values in Table II), whereas geometrical arguments yield a limit $\Lambda_\infty = 5/36$ for very large f .

To access the thermodynamics of the mixture, we solve the two-component RY closure, which is reliable for the one component star polymer system [27] and shows spinodal instability in highly asymmetric hard-sphere mixtures [28]. Monte Carlo simulations using the interactions (1)–(4) as inputs and measuring the structure factors at selected thermodynamic points yielded excellent agreement with RY. The thermodynamic consistency of the RY closure is enforced with a single adjustable parameter ξ ; a simple scaling of the form $\xi_{\alpha\beta} = \xi/\sigma_{\alpha\beta}$, ($\alpha, \beta = c, s$) showed only small differences compared to the unscaled form.

The structure of binary mixtures is described by three partial static structure factors $S_{\alpha\beta}(k)$, with $\alpha, \beta = c, s$, obtained from RY. Indication of a demixing transition is the divergence of all structure factors at the long wavelength limit $k \rightarrow 0$, marking the *spinodal line* of the system. It is more convenient to consider the concentration structure factor $S_{\text{con}}(k) = x_s^2 S_{cc}(k) + x_c^2 S_{ss}(k) - 2x_c x_s S_{cs}(k)$, with the concentrations $x_\alpha = N_i/N$, ($\alpha = c, s$), which provides the approach to thermodynamics through [28,29],

$$\lim_{k \rightarrow 0} S_{\text{con}}(k) = k_B T \left[\frac{\partial^2 g(x_c, P, T)}{\partial x_c^2} \right]^{-1}, \quad (5)$$

where $g(x_c, P, T)$ is the Gibbs free energy $G(x_c, N, P, T)$ per particle, and P denotes the pressure of the mixture. If $g(x_c)$ has concave parts, the system phase separates and the bound-

TABLE II. Fit parameters Λ, κ, τ for the effective star-wall interaction of Eq. (4) and the star-star interaction of Eq. (3) obtained from molecular simulation. R_d is the nonvanishing core radius of one simulated star.

f	$\Lambda(f)$	$\kappa\sigma_s$	$\tau\sigma_s$	R_d/σ_g
2	0.46	0.58	1.03	0.04
6	0.34	0.73	1.14	0.03
16	0.28	0.75	–	0.04
32	0.24	0.84	–	0.06

aries are calculated by the common tangent construction on the $g(x_c)$ versus x_c curves. The results obtained are shown in Figs. 3 and 4.

Inside the spinodal line, the limits $S_{\alpha, \beta}(k \rightarrow 0)$ attain unphysical, negative values associated with the physical instability of the mixture against phase separation. Consequently, a solution of the integral equations is not possible there and above the critical pressure P^* , $S_{\text{con}}(x_c, k=0)$ is unknown in some interval $\Delta x_c(P)$. Thus, it is necessary to interpolate $S_{\text{con}}(x_c, k=0)$ in order to perform the integration of Eq. (5). In the vicinity of the critical point $\eta_c^* \approx 0.3$, the missing interval Δx_c is very small and the interpolation is reliable. Here the binodals should be accurate, while for higher pressures (packing fractions $\eta_c < \eta_c^*$ and $\eta_c > \eta_c^*$) the binodals are more approximate but show reasonable behavior. For highly asymmetric systems ($q \leq 0.18$) it becomes more and more difficult to get solutions of the integral equations in the vicinity of the spinodal line and the calculation of binodals was not possible.

The results in Figs. 3 and 4 show that theory and experiment are in good agreement. This is brought about *without* the use of any free parameters in the former, that would allow for a rescaling of sizes or densities. In particular, the same trends are found as functions of the system parameters f and q . By increasing f at fixed q (Fig. 3), the demixing transition moves to lower star packing fractions η_s and the curves become flat. The most important observation from the

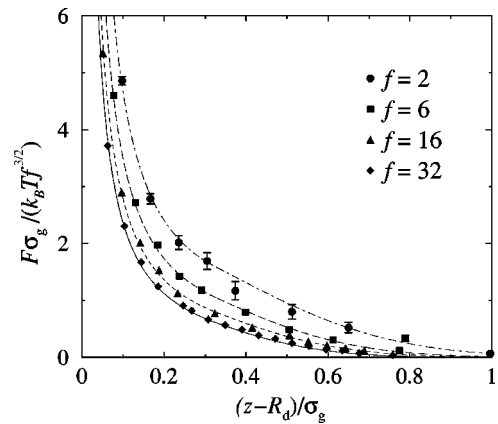


FIG. 2. Effective force between an isolated star polymer and a hard flat wall ($q=0$) for arm numbers $f=2, 6, 16$, and 32 . z is the distance from the star center to the surface of the wall. Theoretical curves from Eq. (4) were compared to computer simulation data (symbols) to obtain the prefactor Λ and the decay parameter κ . For better comparison we divided the force by $f^{3/2}$.

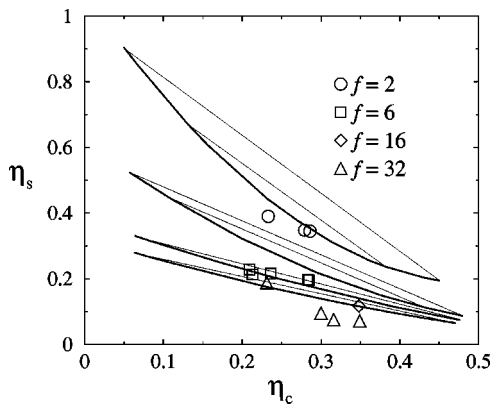


FIG. 3. Binodal lines for the mixing-demixing transition in star-polymer-colloid mixtures for different arm numbers $f=2,6,16,32$ (from top to bottom) and size ratio $q \approx 0.49$. Symbols mark experimental results compared with theory (lines) for $q=0.50$. The thin straight lines are tielines.

results shown in Fig. 3 is that the $f=2$ and $f=32$ mixtures show qualitatively the same phase behavior, i.e., a phase diagram with gas-liquid coexistence. From this point of view, a colloid+32-arm star mixture still resembles a simple colloid-polymer mixture rather than BHS. However, it is surprising that the phase boundary *drops* with increasing star functionality. Apparently, 32-arm stars are more efficient depletants than linear polymers.

When q is decreased but f remains fixed (Fig. 4), again a motion of the binodals to lower η_s is observed. This trend is *opposite* to the one predicted by the AO model [see Figs. 2(e) and 2(f) in Ref. [1]]. The phase separation is not a simple hybrid between the AO and the hard sphere mixture but show an alternative behavior that one could trace back to nonadditivity. A careful mapping of the current system into a

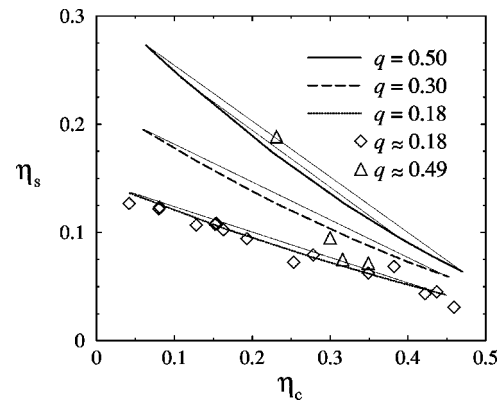


FIG. 4. Same as in Fig. 3 for an arm number $f=32$ and different size ratios q .

nonadditive mixture would therefore be of interest. Yet, in view of the fact that the star-star and the cross interactions display soft tails, such a mapping is not straightforward and attempts in this direction are the subject of current investigations.

The absolute thermodynamic stability of the liquid phase will be influenced by the competing crystal phases that may preempt the demixing transition. Here, the exciting possibility opens up that for size ratios $q \geq 0.5$ and $f > 32$, colloid-star superlattices similar to those seen in the BHS may be stable, whereas for smaller size ratios and/or functionalities, the crystals would be of the ‘‘sublattice-melt’’ type. In this context, it may be significant that stars crystallize only when $f > 34$ [22].

We thank M. Schmidt, A. A. Louis, R. Finken, and A. Lang for useful discussions and the DFG for support within the SFB 237. J.S. is supported by the DFG and A.B.S. by NASA.

-
- [1] S.M. Ilett *et al.*, Phys. Rev. E **51**, 1344 (1995).
 [2] A. Moussaïd *et al.*, Phys. Rev. Lett. **82**, 225 (1999).
 [3] H.N.W. Lekkerkerker *et al.*, Europhys. Lett. **20**, 559 (1992).
 [4] M. Dijkstra *et al.*, J. Phys.: Condens. Matter **11**, 10 079 (1999).
 [5] A.A. Louis *et al.*, Europhys. Lett. **46**, 741 (1999).
 [6] M. Fuchs and K.S. Schweizer, Europhys. Lett. **51**, 621 (2000).
 [7] A.A. Louis *et al.*, Phys. Rev. Lett. **85**, 2522 (2000).
 [8] P.G. Bolhuis *et al.*, J. Chem. Phys. **114**, 4296 (2001).
 [9] M. Dijkstra *et al.*, Phys. Rev. E **59**, 5744 (1999).
 [10] R. Seghrouchni *et al.*, Europhys. Lett. **42**, 271 (1998).
 [11] C.N. Likos *et al.*, Phys. Rev. Lett. **80**, 4450 (1998).
 [12] A. Jusufi *et al.*, Macromolecules **32**, 4470 (1999).
 [13] A. Jusufi *et al.*, e-print, cond-mat/0012384.
 [14] L. Antl *et al.*, Colloids Surface **17**, 67 (1986).
 [15] J. Allgaier *et al.*, Macromolecules **32**, 3190 (1999).
 [16] N. Hadjichristidis and L.J. Fetters, Macromolecules **13**, 191 (1980).
 [17] G.S. Grest *et al.*, Adv. Chem. Phys. **XCIV**, 67 (1996).
 [18] The neutron scattering was performed in *d*-cis-decalin using D11 (ILL, Grenoble, France); see *experimental report 9-11-684* (2000).
 [19] J. Stellbrink *et al.* (unpublished).
 [20] W.C.K. Poon *et al.*, Faraday Discuss. **101**, 65 (1995).
 [21] F.A. Rogers and D.A. Young, Phys. Rev. A **30**, 999 (1984).
 [22] M. Watzlawek *et al.*, Phys. Rev. Lett. **82**, 5289 (1999).
 [23] M. Daoud and J.P. Cotton, J. Phys. (Paris) **43**, 531 (1982).
 [24] B. Krüger *et al.*, J. Phys. (Paris) **50**, 3191 (1989).
 [25] T.A. Witten and P.A. Pincus, Macromolecules **19**, 2509 (1986).
 [26] P. Pincus, Macromolecules **24**, 2912 (1991).
 [27] M. Watzlawek *et al.*, J. Phys.: Condens. Matter **10**, 8189 (1998).
 [28] T. Biben and J.-P. Hansen, Phys. Rev. Lett. **66**, 2215 (1991).
 [29] A.B. Bhatia and D.E. Thornton, Phys. Rev. B **2**, 3004 (1970).